Work Report

Zhuoran Qiao

October 14, 2018

1 Introduction

1 Developed a genetic algorithm based approach to simulate kinetics of co-transcriptional folding.

2 Tested effect of folding rate variation on folding population dynamics and $p_{unbound}$.

2 Progress

2.1 Framework

Various algorithms or programs have been developed to predict RNA folding pathway ultilizing force-field based simulations[1] and multiple sampling methods based on Monte Carlo trajectories[2][3] or coarse graining of energy landscape built on Markov state model[**?**][4]. Those present methods have succeeded in revealing multiscale dynamic events during RNA folding, however are either designed for only predicting annealing dynamics or limited to RNA segments with length up to hundred bases. To quantitatively predict folding dynamics coupled with transcription, we developed GenoFold, a genetic algorithm and chemical Master equation based approach, which is capable of capturing kilobase level kinetics. Our method is built on two following assumptions:

1 All populated RNA secondary structures (SS) are linkage of locally optimal or sub-optimal structures at various folding sites;

2 Global structural rearrangement of a partial RNA segment is permitted only if it's folding to the optimal SS on that segment.

Formally, we denote a domain $D_{A,\,B}$ as a segment between base A and B that all contacts on that segment are local. For simplicity, we denote **foldon** as domains with optimal secondary structures: $D^{foldon}_{A,\,B}$ = MFE(sequence[A,B]). Note that $'.'$ is a trival example of foldon. Our assumption 1 can be rewritten as

$$D_{A,\,B} = D^{foldon}_{A,i_1} \oplus D^{foldon}_{i_1,i_2} \oplus ... \oplus D^{foldon}_{i_n,B} \tag{1}$$

Where $\oplus$ represents a link operation. Note that all structural information of $D_{A,\,B}$ is encoded by the sequential representation $[A,\, i_1,\, ...,\, i_n,\, B]$; as a foldon is also a linkage of smaller foldons, there could be multiple way to represent $D_{A,\,B}$. Here we introduce **Irreducible Foldon Representation** (IFR) to be the sequential representations for which linkage of every adjacent foldons is not another foldon: $\forall k$, $D^{foldon}_{i_k,i_{k+1}} \oplus D^{foldon}_{i_{k+1},i_{k+2}} \neq D^{foldon}_{i_k,i_{k+2}}$. Then the sufficient and necessary condition for structural rearrangement is

$$\begin{gathered}\langle D^u_{A,\,B}|\hat{\mathbf{T}}|D^v_{A,\,B}\rangle \neq 0 \text{ if and only if } \exists\, i,\, j \text{ satisfies} \\ i,\, j \in D^u_{A,\,B}.\text{IFR},\; i,\, j \in D^v_{A,\,B}.\text{IFR}; \\ D^u_{A,\,i} = D^v_{A,\,i},\; D^u_{j,\,B} = D^v_{j,\,B}; \\ D^u_{i,\,j} = D^{foldon}_{i,\,j} \text{ or } D^v_{i,\,j} = D^{foldon}_{i,\,j}. \\ \text{Then } \langle D^u_{A,\,B}|\hat{\mathbf{T}}|D^v_{A,\,B}\rangle = \langle D^u_{i,j}|\hat{\mathbf{T}}|D^v_{i,j}\rangle.\end{gathered}$$

2.2 Folding pathway identification & Rate calculation

Given two domains between which rearrangement is allowed, the task is to compute forward and backward rate constant linking each other. Methods to rigorously calculate the maximum likelihood pathway between arbitrary RNA structrues have been reported[**?**]; here we proposed a computationally feasible approach: the forward free energy barrier is estimated by sum up all free energy associated with old stacks unzipping and new loop forming; then rate constant $k_{uv} = \langle D^u_{A,\,B}|\hat{\mathbf{T}}|D^v_{A,\,B}\rangle$ is calculated by Arrhenius approximation $k_{uv} = k_0 \exp\left[-\frac{1}{RT}(\Delta G^{Stack}_u + \Delta G^{Loop}_v)\right]$. 'New' and 'old' helices are identified by comparing elementary domains (defined as domains that cannot be decomposed to smaller valid domains) between reactant and product domains; identical elementary domains are excluded.

2.3 Algorithm procedure

During every iterative elongation step, an active species pool of strands with unique SS and diffrent population is updated. New candidate strands $D^{Candidate}_{0,\,L+\Delta L}$ with length $L + \Delta L$ are generated by a recombination process: for every old strand $D^{Strand}_{0,\,\mathrm{L}}$, all indices in its IFR is identified as possible rearrangement site, then its child strands is generated by linking partial domains $D^{Strand}_{0,\,\mathrm{Site}}$ with a foldon $D^{foldon}_{\mathrm{Site},L+\Delta L}$ that terminated at $L + \Delta L$.

We assume that elongation will not change the inital population distribution of secondary structures: child strands with the exact parental SS on $[0, L]$ ($D^{child}_{0,L+\Delta L} = D^{strand}_{0,L} \oplus D^{foldon}_{L,L+\Delta L}$) will also inherit the population of their parents.

After structual generation the rate matrix among all candidate strands within the new active species pool is calculated (see part 2.2). Then the population distribution of strands after elongation is computed by propagate the chemical master equation.

For the sake of computational efficiency, we introduce a cutoff N as the size limit of the active species pool. After each elongation step, we impose a selection sweep on all active strands; species with top N fitness is reserved. In the current edition, we simply used population as the fitness function. Population of remaining strands within the active pool is renormalized after selection.

Pseudocodes of GenoFold simulation procedure are as follows (Algorithm 1):

2.4 Test results

The only remaining free parameter to be determined is k_0/k_T, the ratio of pre-exponential factor in Arrhenius rate formulation for folding and trancription rate ($nt \cdot s^{-1}$). I tuned k_0/k_T from 10^1 to 10^{15} and obtained the data for $k_0/k_T = \infty$ by calculating stationary distribution ($\frac{1}{Q}\exp(-G_i)$) after every elongation step for strand i in active pool.

Population analysis For folA-WT four predominant local folding motifs within SD sequence are identified. Figure 1 shows exemplary secondary structures containing these motifs; figure 2 shows evolution of these structure motifs during co-transcriptional folding with different k_0/k_T. Identical motifs are marked by the same color as in figure 1. Surprisingly we noticed that when $k_0/k_T = \infty$, exchange between energetially favorable motifs was very frequent at early stage of transcription, indicating the sensitivity of local structures on long-range contacts. We

Algorithm 1 Co-transcriptional folding elongation procedure

```
Initalize ActivePool
while sequence length > current length do
    OldPool ← ActivePool
    renew ActivePool
    Current length ← Current length + $dL$
    dt ← $dL/k_T$                                        ▷ Transcription time
    for left boundary ∈ {0, dL, 2dL, ..., Current length - dL} do    ▷ Get all new foldons
        $D^{foldon}_{\text{left boundary, Current length}}$ ← numpy.mfe(sequence[left boundary, Current length])
    end for
    for Strand ∈ OldPool do                              ▷ Recombination
        for Site ∈ Strand.IFR do
            $D^{Candidate}_{\text{0,Current length}} \leftarrow D^{Strand}_{\text{0, Site}} \oplus D^{foldon}_{\text{Site, Current length}}$
            if $D^{Candidate}_{\text{0,Current length}}$ ∈ ActivePool then
                update $D^{Candidate}_{\text{0,Current length}}$.IFR
            else
                add $D^{Candidate}_{\text{0,Current length}}$ to ActivePool
            end if
            if site = Current length $-\, dL$ then
                $\langle \text{ActivePool.}\mathbf{population}\,|D^{Candidate}_{\text{0,Current length}}\rangle \leftarrow \langle \text{OldPool.}\mathbf{population}\,|D^{Strand}_{\text{0, Site}}\rangle$
            end if
        end for
    end for
    for $D^{\text{u}}_{\text{0,Current length}} \neq D^{\text{v}}_{\text{0,Current length}}$ ∈ ActivePool do    ▷ Calculate new rate matrix
        calculate $D^{u}_{\text{rearrange}}$, $D^{v}_{\text{rearrange}}$    ▷ Find all helices involved in rearrangement
        $\langle D^{u}_{\text{rearrange}}|\hat{\mathbf{T}}|D^{v}_{\text{rearrange}}\rangle \leftarrow k_0 \exp\Big(-\frac{1}{RT}(\Delta G^{Stack}_{u} + \Delta G^{Loop}_{v})\Big)$
    end for
    $\langle \text{ActivePool.}\mathbf{population}\,| \leftarrow \langle \text{ActivePool.}\mathbf{population}\,|\exp\Big(t \times \hat{\mathbf{T}}\Big)$    ▷ Master equation
    reserve top $N$ populated strands in ActivePool      ▷ Selection
    renormalize $\langle \text{ActivePool.}\mathbf{population}\,|$
end while
```

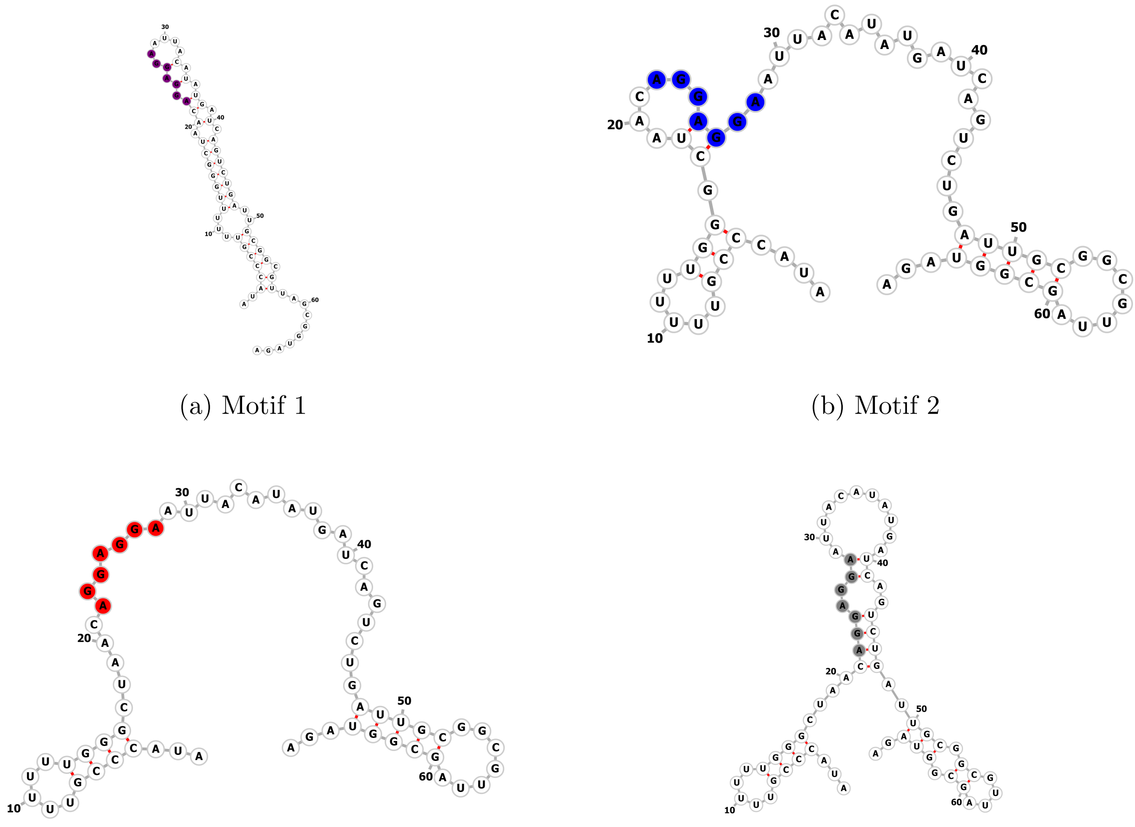

(a) Motif 1

(b) Motif 2

(c) Motif 3

(d) Motif 4

Figure 1: Exemplary ss containing folding motifs within folA-WT Shine-Dalgarno sequence

also noticed that motif predominance after transcription strongly depended on folding rate, reiterating the importance of time scale in the folding problem.

$p_{unbound}$ analysis We calculated $p_{unbound}$ with respect to transcription time and k_0/k_T (Figure 3-10). As a data test we used nupack.ppairs to calculate equilibrium $p_{unbound}$ for all truncated sequences. Deviation of asymptotic behavior of model from equilibrium value is possiblly due to the limited set of foldons (only used mfe to obtain current results).

2.5 Model optimization

We observed that our model tends to overesitimate the flucuation of average $p_{unbound}$ when $k = \infty$, and some kinetic patterns were lost (for bases -11, -12 and -14). Specifically we found that for base -8 and base -9, our model gave identical results while for equilibrium nupack.ppairs calculation there was a overall upshift of $p_{unbound}$.

Then we examined sub-optimal structures using nupack.subopt for sequence truncated at 150 nt, and found two tentative kinetically important structures between which free energy difference is 0.7 kcal (Figure 11). Coexistence of those sub-optimal structures instead of only the minimum free energy structure will possibly result in similar population dynamics as above but different $p_{unbound}$ at single base resolution. We also noticed that for mininum free energy motifs, base -11, -12 and -14 shared the same pairing patterns, meaning that $p_{unbound}$ for such bases has no response to motif population dynamics.

From above results, we suggest that optimizing foldon collections by incorporate sub-optimal structures with a energy gap of 1cal/mol could improve the predictibility of our model.

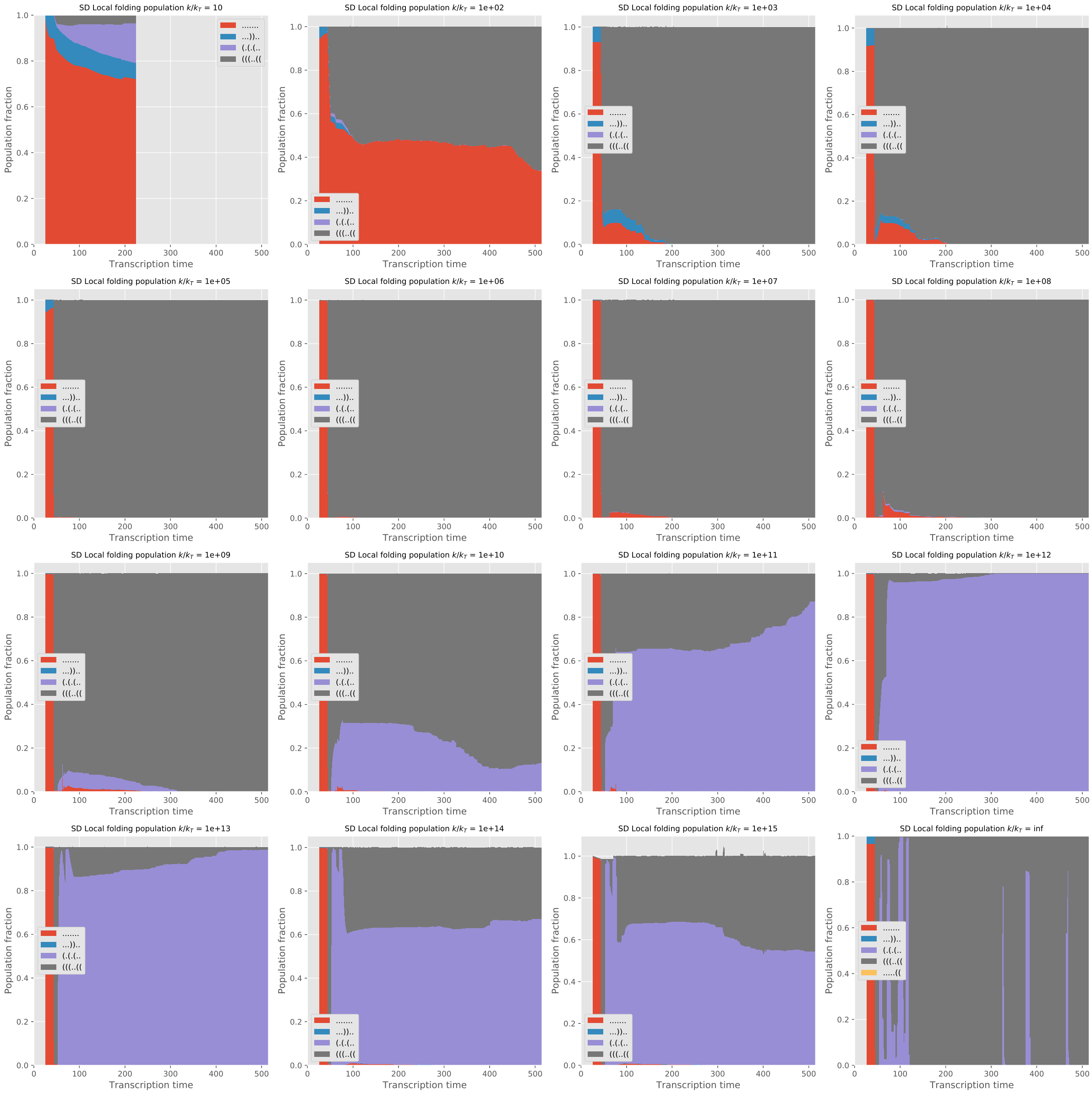

Figure 2: Population dynamics of four structrual motifs during co-transcriptional folding.

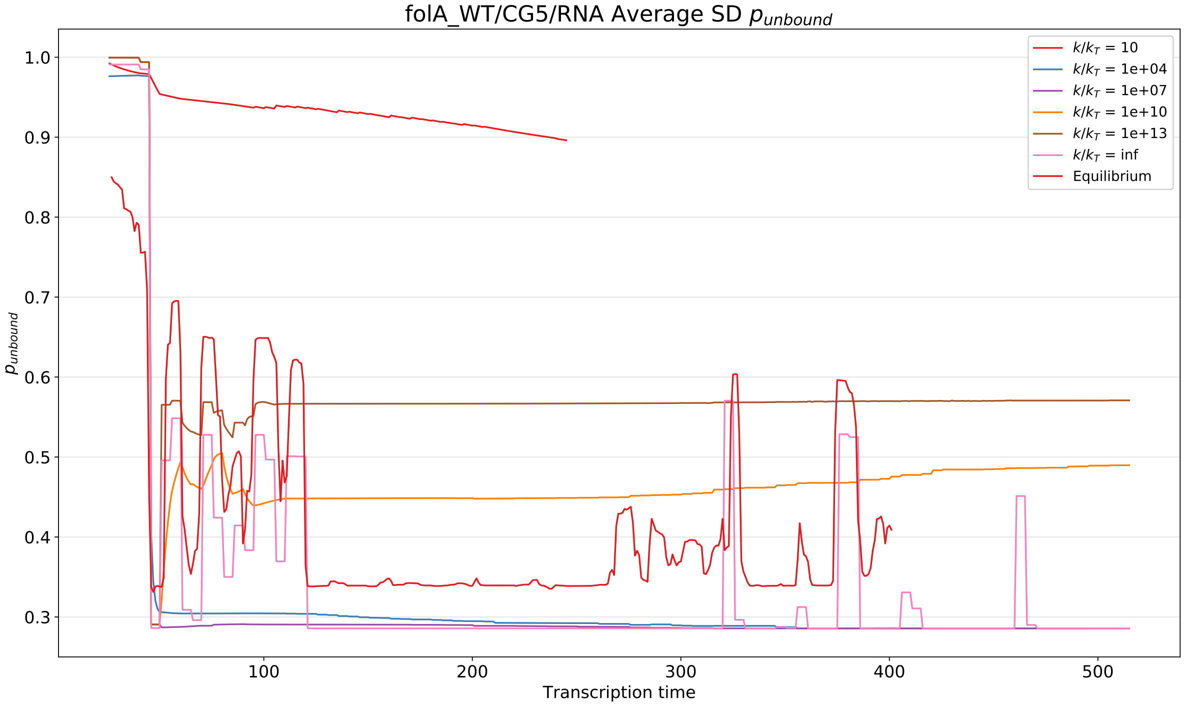

Figure 3: Average $p_{unbound}$ of SD sequence during transcription.

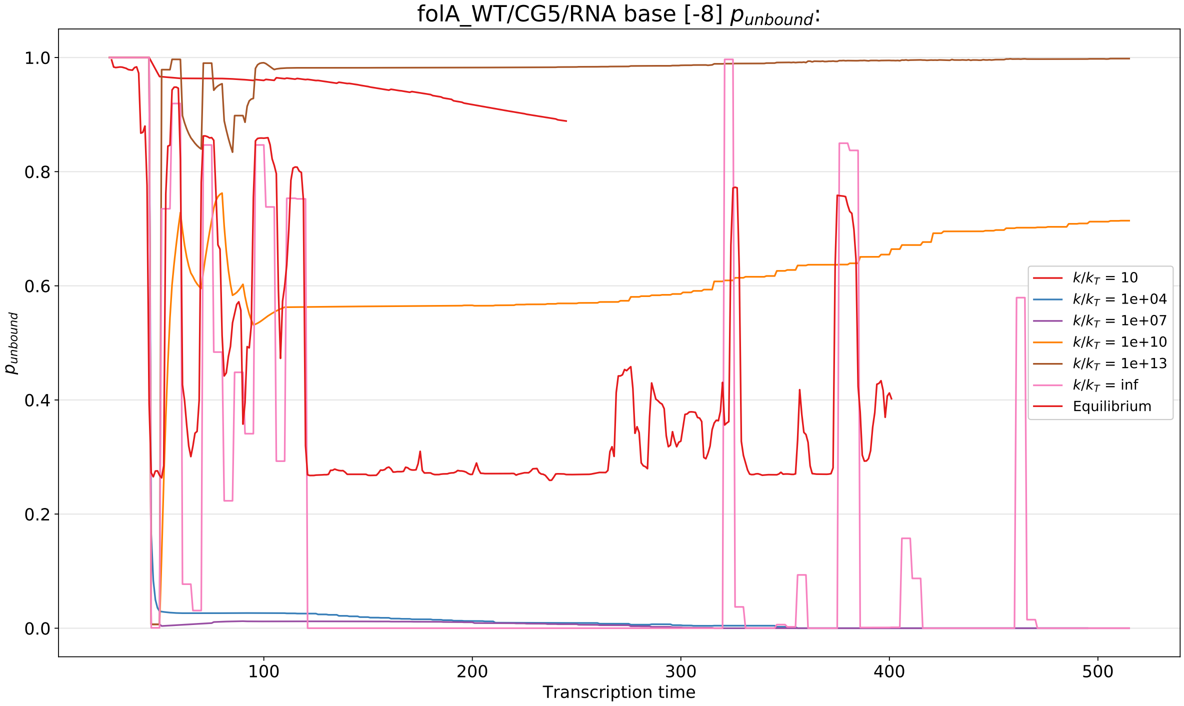

Figure 4: $p_{unbound}$ of base -8 during transcription.

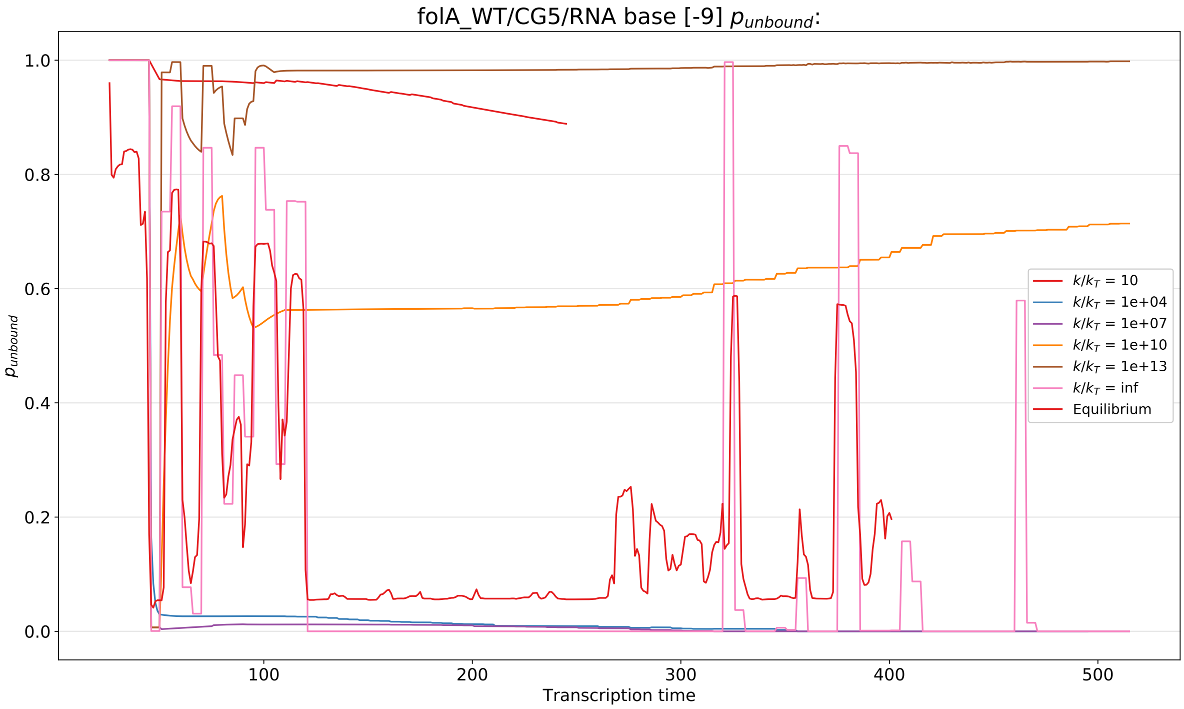

Figure 5: Same as above, base -9.

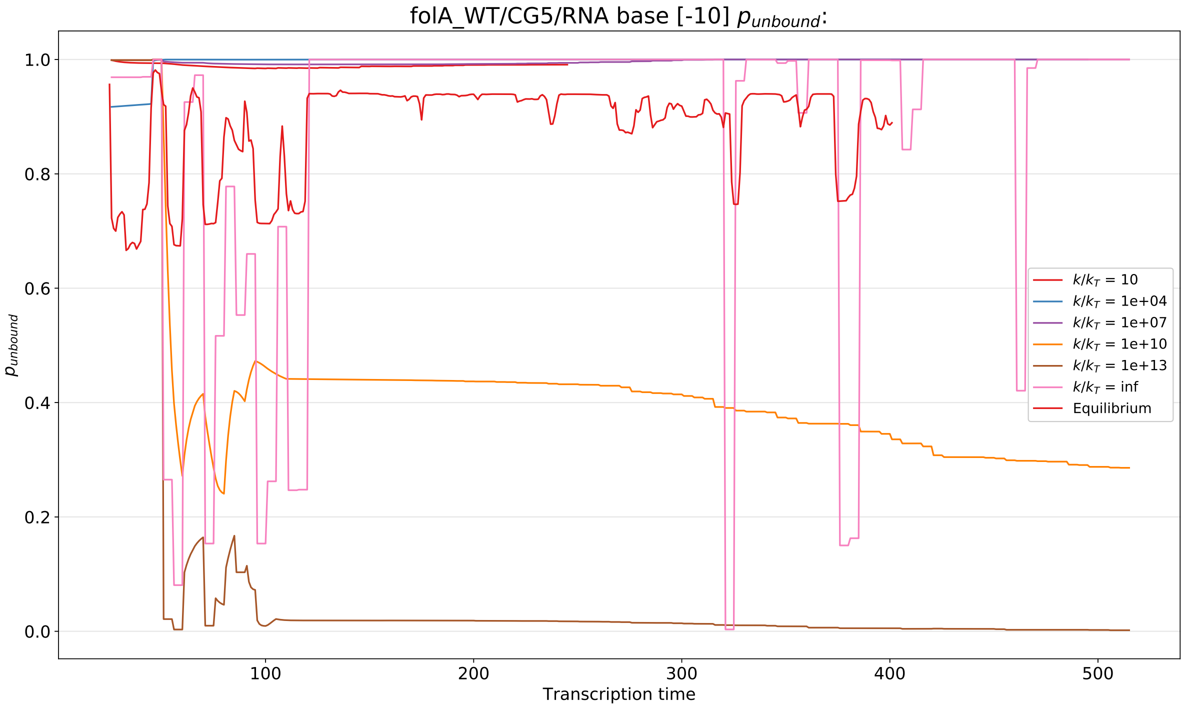

Figure 6: Same as above, base -10.

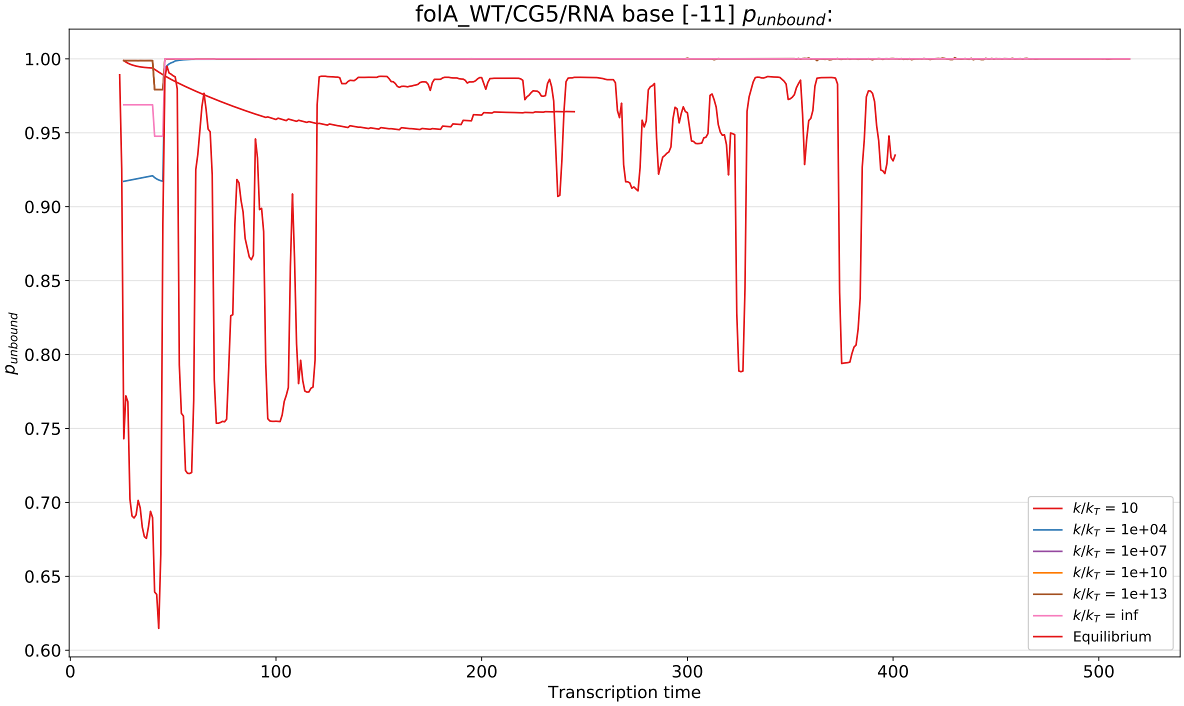

Figure 7: Same as above, base -11.

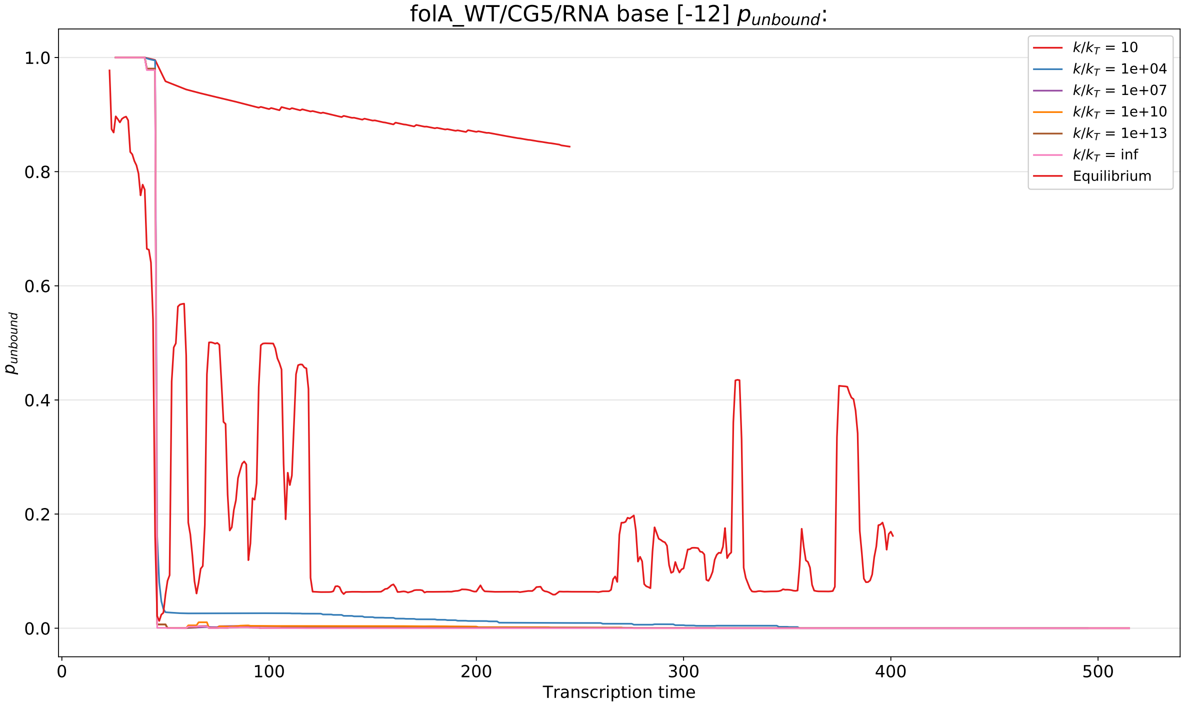

Figure 8: Same as above, base -12.

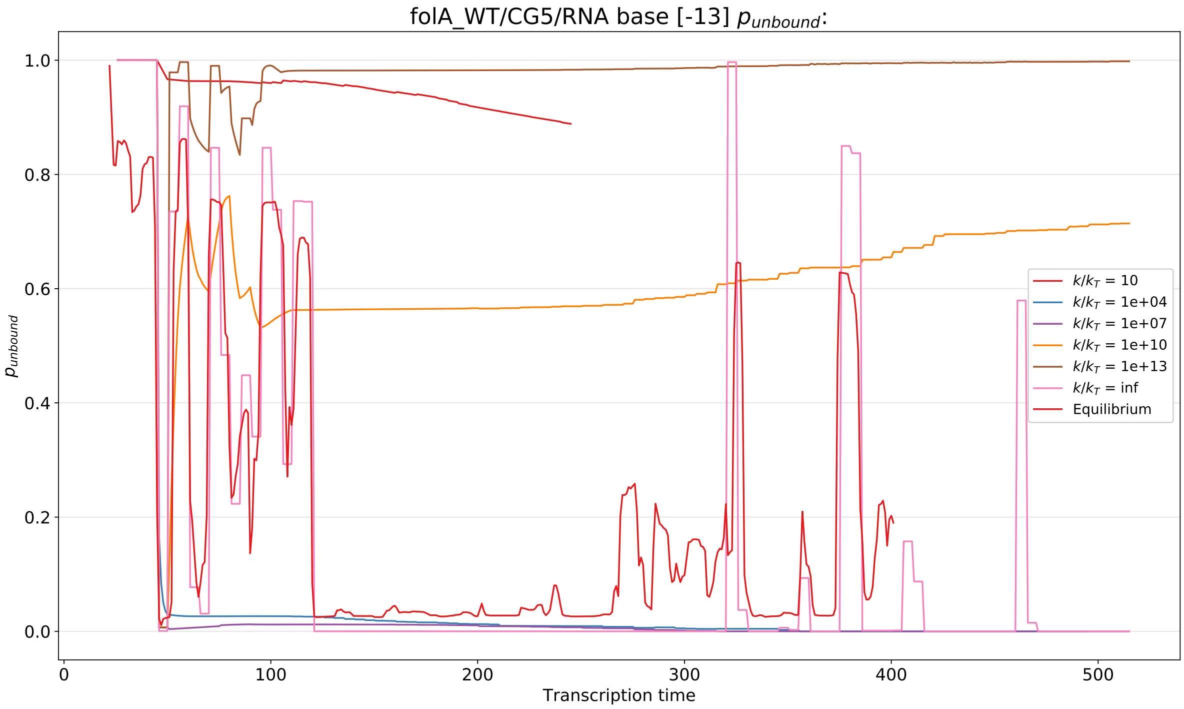

Figure 9: Same as above, base -13.

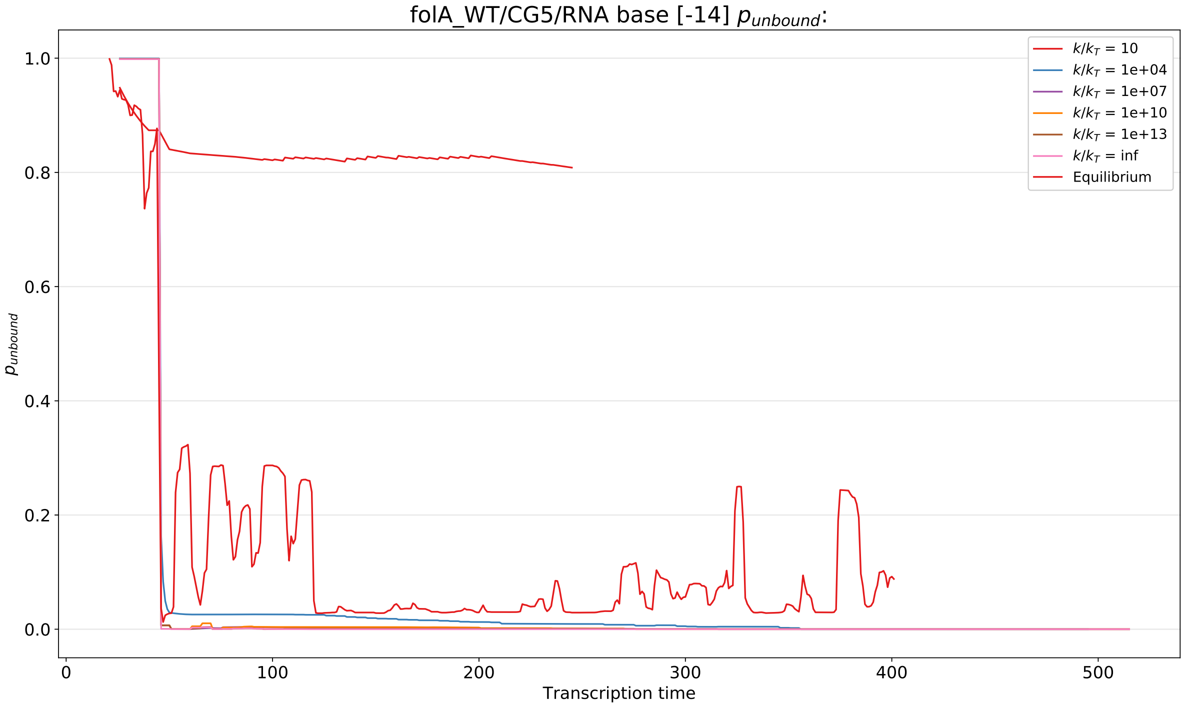

Figure 10: Same as above, base -14.

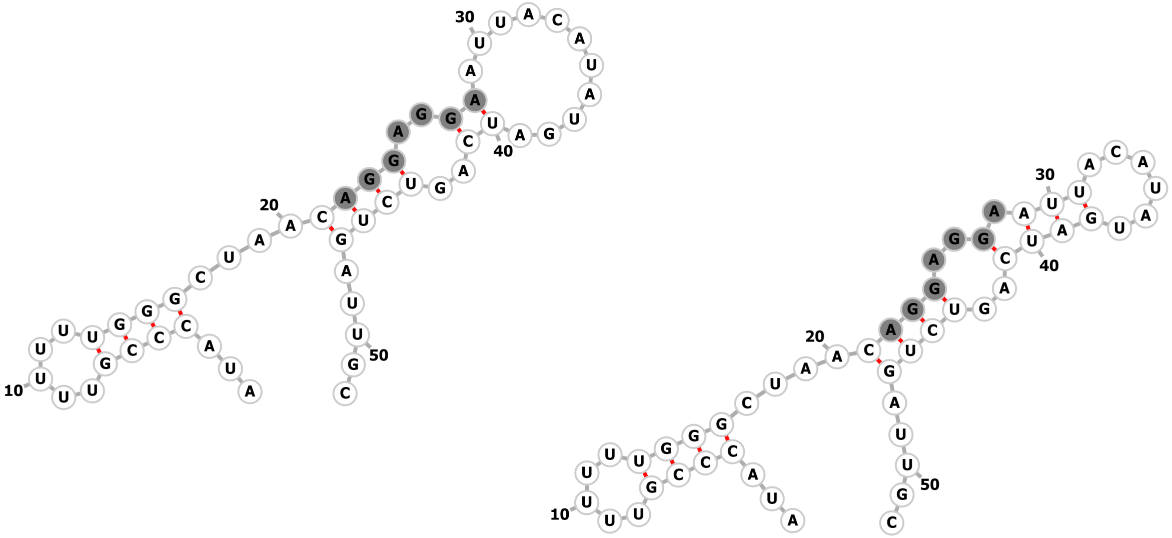

Figure 11: Tentative kinetically important sub-optimum structures (dG = 0.7 kcal/mol).

3 Future plan

1 Optimize GenoFold by including sub-optimal foldons for structure generation (in progress);

2 Bioinformatic analysis of translation initiation rate along synonymous mutants based on prediction data.

References

[1] Raviprasad Aduri, Brian T. Psciuk, Pirro Saro, Hariprakash Taniga, H. Bernhard Schlegel, and John SantaLucia. AMBER force field parameters for the naturally occurring modified nucleosides in RNA. *Journal of Chemical Theory and Computation*, 3(4):1464–1475, 2007.

[2] Alexander P. Gultyaev, F. H.D. Van Batenburg, and Cornelis W.A. Pleij. The computer simulation of RNA folding pathways using a genetic algorithm. Technical Report 1, 1995.

[3] Peter Clote and Amir H. Bayegan. RNA folding kinetics using Monte Carlo and Gillespie algorithms? Technical report, 2017.

[4] Tingting Sun, Chenhan Zhao, and Shi Jie Chen. Predicting Cotranscriptional Folding Kinetics for Riboswitch. *Journal of Physical Chemistry B*, 2018.